

c.2

NACA RM 56C20



# RESEARCH MEMORANDUM

CORRELATION OF CREEP-BUCKLING TESTS WITH THEORY

By Sharad A. Patel, Joseph Kempner, Burton Erickson,  
and Abol H. Mobassery

Polytechnic Institute of Brooklyn

EXACT COPY

MAY 23 1956

RECEIVED

1956

ROBERTS FIELD, VIRGINIA

**NATIONAL ADVISORY COMMITTEE  
FOR AERONAUTICS**

WASHINGTON

May 23, 1956

## NATIONAL ADVISORY COMMITTEE FOR AERONAUTICS

## RESEARCH MEMORANDUM

## CORRELATION OF CREEP-BUCKLING TESTS WITH THEORY

By Sharad A. Patel, Joseph Kempner, Burton Erickson,  
and Abol H. Mobassery

## SUMMARY

The results of short-time creep-buckling and creep-bending tests of 2024-T4 aluminum-alloy columns of slenderness ratio 111 are presented. The tests were performed at 600° F, and strain measurements were taken with high-temperature electric-resistance strain gages. A description of the development of the gages is given in an appendix. The column tests show that the critical time decreases much more rapidly with increasing load than with increasing initial deviation from straightness. The bending tests indicate that the steady creep rate of the curvature is a simple power function of applied moment. These latter results, together with a previously derived creep-buckling theory, are used to develop a semiempirical formula suitable as a guide for the determination of the critical time for columns.

## INTRODUCTION

When a load-carrying structure is used at elevated temperatures, its structural elements deform with time even though the external loads may not change. If the structure contains components which are subjected to compressive loads, the danger of a local or general instability exists because of the interaction between the loads and creep deformations. The need for suitable design criteria covering such failures is apparent. Unfortunately, such problems are extremely complicated and generally not amenable to simple calculations. Such is the column problem. Notwithstanding, several more or less approximate column creep-buckling theories have been published in the past few years (for example, refs. 1 to 6). Some appropriate column tests have also been reported (for example, refs. 4 and 7 to 11). In reference 10 a fairly comprehensive test program, the results of which were presented in the light of the theoretical results of reference 2, facilitated the construction of column curves for 7075-T6 aluminum-alloy columns. These curves appear to be satisfactory for design purposes in the temperature range 300 to 600° F.

The present report represents an extension of references 11 and 5, respectively, inasmuch as it reports on the results of a series of creep-buckling tests on 2024-T4 aluminum-alloy columns and applies the results of the creep-buckling theory described in reference 5. Data obtained from creep-bending tests and used in the correlation of column tests and theory are also presented. In the column and beam tests, high-temperature electric-resistance strain gages were used to measure strain. The development of these gages is described in the appendix. A semi-empirical formula is derived which may serve as a guide for determining the manner in which the critical time of a column depends upon load, initial deviation from straightness, and the physical and geometric properties of a column.

This investigation was carried out under the sponsorship and with the financial assistance of the National Advisory Committee for Aeronautics. The authors are grateful to Professor N. J. Hoff for his valuable suggestions and to Messrs. Francis W. French and Samuel Ledermann for their assistance in the test program.

#### SYMBOLS

A	area of cross section of column
$a_n$	amplitude of nth Fourier component of initial deviation from straightness
E, $E_T$	modulus of elasticity at room temperature and at elevated temperature, respectively
$E_1$	creep constant
$e_n = a_n/\rho$	
$e_{1\_hot}$	value of $a_1/\rho$ determined at elevated temperature
$f_{T_0}$	ratio of total midpoint deflection to column depth at $t = 0$ , $(a_1/h^*) / \left[ 1 - (\bar{\sigma}/\sigma_E) \right]$
h	depth of cross section of column
$h^*$	depth of idealized H-section equivalent of rectangular section, $h/\sqrt{3}$

I	least moment of inertia of rectangular cross section
k, m	creep constants
L	column length
M	bending moment
n	integer
P	axial load on column
$P_E$	Euler load
R	radius of curvature
t	time
$t_{cr}$	critical time
$t_1$	time at which $z = 1/2$
$w_i$	initial deviation from straightness
$w(t)$	deflection due to loads
$\bar{w}(t)$	amplitude of $w(t)$
$w^*$	total midpoint deflection immediately prior to collapse
x	axial coordinate
z	ratio of total midpoint deflection to column depth at any time t
$\alpha$	ratio of applied load to Euler load or ratio of average axial elastic strain to Euler strain, $P/P_E$ or $\bar{\epsilon}/\epsilon_E$
$\epsilon$	strain, positive in compression
$\epsilon_E$	Euler strain, $(\pi\rho/L)^2$
$\bar{\epsilon}$	average elastic strain across column depth, $P/AE$
$\Delta\epsilon$	difference in strain on convex and concave surfaces of beam or column

$\Delta\epsilon_{av}$	average of $\Delta\epsilon$ taken over central two-thirds of column
$\lambda$	creep constant
$\rho$	radius of gyration of rectangular cross section, $h/2\sqrt{3}$
$\sigma$	stress, positive in compression
$\bar{\sigma} = P/A$	
$\sigma_E$	Euler stress
$\tau$	nondimensional time parameter
$\tau_{cr}$	critical value of time parameter
$\tau_1$	value of time parameter corresponding to $z = l/2$

#### COLUMN TESTS

The results of two series of elevated-temperature tests performed on columns fabricated from 2024-T4 aluminum alloy were presented in an earlier report (ref. 11). Except for the technique described therein for the determination of the initial deviations from straightness, the method of testing and the testing apparatus used in the present (third) series of tests were the same and, hence, are not described. Determination of the initial deviations from straightness in the tests reported here was accomplished at room and elevated temperatures with the aid of the high-temperature electric-resistance strain gages described in the appendix.

#### Determination of Initial Deviation From Straightness

The initial deviation from straightness can be represented by the Fourier series

$$w_1 = \sum_{n=1}^{\infty} a_n \sin(n\pi x/L) \quad (1)$$

in which  $w_1$  represents the initial deviation of the center line of the column from the line of action of the axial load,  $a_n$  is the amplitude

of the  $n$ th Fourier component, and  $x$  and  $L$ , respectively, are the coordinate and length measured along a straight line from one knife edge to the other (fig. 1). If an axial compressive load is applied to an elastic, simply supported column of rectangular cross section, the difference in the strain on the convex and concave sides is, from reference 11,

$$\Delta\epsilon = -(\pi/L)^2 h \alpha \sum_{n=1}^{\infty} \left[ \frac{n^2}{(n^2 - \alpha)} \right] a_n \sin(n\pi x/L) \quad (2)$$

in which  $h$  is the depth of the cross section,  $\alpha$  is the ratio of the applied load  $P$  to the Euler load  $P_E = (\pi/L)^2 EI$ ,  $E$  is the elastic modulus, and  $I$  is the least moment of inertia of the cross section of the column. The average elastic strain across the depth is

$$\bar{\epsilon} = P/AE \quad (3)$$

in which the strain is considered positive in compression and  $A$  is the cross-sectional area. Since the depth of the rectangular cross section is related to the radius of gyration  $\rho$  according to  $h = 2\sqrt{3}\rho$  and since the Euler strain is given by  $\epsilon_E = (\pi\rho/L)^2$ , equation (2) can be expressed in terms of strains as

$$\Delta\epsilon = 2\sqrt{3} \alpha \epsilon_E \sum_{n=1}^{\infty} \left[ \frac{n^2}{(n^2 - \alpha)} \right] e_n \sin(n\pi x/L) \quad (4)$$

in which  $e_n = a_n/\rho$  and  $\alpha = P/P_E = \bar{\epsilon}/\epsilon_E$ .

In order to correlate the creep-buckling characteristics of columns with the amplitude  $e_1$  of the first harmonic of the initial deviation, it is desirable that this quantity be determined very accurately. In the present work this is accomplished with the use of suitable-gage-length high-temperature strain gages (see appendix). These gages are attached to the column in such a manner as to measure the change in the extreme fiber lengths over the central two-thirds of the column length. The average strain difference over this length is then

$$\Delta\epsilon_{av} = (3/2L) \int_{L/6}^{5L/6} \Delta\epsilon \, dx \quad (5)$$

Equations (4) and (5) yield

$$\Delta\epsilon_{av} = -(6/\pi) \sqrt{3} \alpha \epsilon_E \sum_{n=1}^{\infty} \left[ n / (n^2 - \alpha) \right] e_n \sin(n\pi/2) \sin(n\pi/3) \quad (6)$$

It may be noted that those harmonics for which  $n$  is a multiple of 2 or 3 do not contribute to  $\Delta\epsilon_{av}$ . Thus,  $e_2$ ,  $e_3$ ,  $e_4$ ,  $e_6$ , and so forth do not affect the calculations. Hence, if the applied load is not too difficult from the Euler load, all harmonics other than the first will contribute insignificantly; and, therefore, the average strain difference can be approximated by

$$\Delta\epsilon_{av} = -(9/\pi) \left[ \alpha / (1 - \alpha) \right] \epsilon_E e_1 \quad (7)$$

This relation can be expressed in a form analogous to that used for a Southwell plot:

$$\Delta\epsilon_{av} = \epsilon_E \left( \Delta\epsilon_{av} / \bar{\epsilon} \right) + (9/\pi) \epsilon_E e_1 \quad (8)$$

in which  $\Delta\epsilon_{av}$  and  $\left( \Delta\epsilon_{av} / \bar{\epsilon} \right)$  are considered as variables; and, hence, the equation is that of a straight line, each point of which corresponds to a given end load. The slope of the line is the critical strain  $\epsilon_E$  and the intercept is proportional to the nondimensional initial deviation amplitude  $e_1$ . Hence, if  $\Delta\epsilon_{av}$  and  $\bar{\epsilon}$  are measured for a series of end loads,  $\epsilon_E$  and  $e_1$  can be determined.

#### Measurement of $\Delta\epsilon_{av}$ and $\bar{\epsilon}$ and Determination of $e_1$

For the experimental determination of the average extreme fiber strains, four high-temperature strain gages, each of whose length was one-third of the column length, were attached to the test specimen as indicated in figure 2(a). In figure 2 the locations of the gages are indicated by the numbers 1 to 4. These gages were connected to a Baldwin SR-4 strain indicator to form a complete four-arm bridge as

shown in figure 2(b). This configuration afforded the direct determination of twice the difference of the average maximum fiber strain; that is,  $2\Delta\epsilon_{av}$ . It also provided for automatic temperature compensation and for maximum output from the bridge. In addition, a switching system enabled the gages to be coupled as indicated in figure 2(c). This arrangement facilitated the measurement of twice the average strain, that is,  $2\bar{\epsilon}$ .

The procedure for the alinement of a column was similar to that described in reference 11. This was always performed at room temperature. The upper pair and lower pair of gages were used separately (fig. 2(a)), and known increments of load were applied to determine whether the two pairs of gages yielded the same average strain  $\bar{\epsilon}$  for a given load. This requirement was met in all tests. To insure symmetry of the deflections, at the load level corresponding to that at which the creep-buckling test was to be conducted the column was alined in such a manner that the upper and lower pairs of gages yielded the same strain difference. During this period of adjustment, the knife-edge supports were set to give strain differences in close accord with those calculated to correspond to a prescribed value of the initial deviation amplitude  $e_1$ .

When the alinement was completed, the circuits were arranged as described previously in order to permit the determination of  $\Delta\epsilon_{av}$  and  $\bar{\epsilon}$ . At room temperature several sets of measurements of these quantities were made for load variations corresponding to  $\alpha = 0.70$  to  $0.95$ , and the results were plotted in accordance with equation (8) to obtain a curve of  $\Delta\epsilon_{av}$  versus  $\Delta\epsilon_{av}/\bar{\epsilon}$ . A typical curve is shown in figure 3. For each column tested, the slope and intercept of the straight-line portion of the corresponding curve of  $\Delta\epsilon_{av}$  versus  $\Delta\epsilon_{av}/\bar{\epsilon}$  were determined by the method of least squares (see eq. (8)). The resulting Euler strain  $\epsilon_E$  and nondimensional initial-deviation amplitude  $e_1$ , so determined, are listed in table 1. It may be noted from equation (8) that, although values of  $\epsilon_E$  depend upon the gage factor, values of  $e_1$  do not, provided all gage factors are identical. Also included in table 1 is the Euler strain calculated from  $\epsilon_E = (\pi\rho/L)^2$ . The test results for  $\epsilon_E$  are seen to be in good agreement with the calculated value. The table also contains values of the initial-deviation amplitude  $e_{1hot}$ , which were determined at the creep-buckling test temperature of  $600^\circ$  F. Because the length of time required to measure strain increments at various load levels would be sufficient to cause considerable creep at  $600^\circ$  F,  $e_{1hot}$  was determined with the aid of equation (7) from a single measured change  $\Delta\epsilon_{av}$  corresponding to the increment in load from preload ( $\alpha = 0.091$ ) to column-test load ( $\alpha = 0.704$ ). Thus, the results obtained for  $e_{1hot}$  cannot be

considered too reliable, even though the effects of many of the higher harmonics are automatically eliminated by the technique employed.

### Results of Creep-Buckling Tests

The results of creep-buckling tests performed on the six columns each of slenderness ratio 111, 12 inches long, and having a cross section of 3/8 by 1/2 inch are presented in table 1 and figures 4 and 5. In each case the test temperature was 600° F and the end load was 774 pounds ( $\alpha = 0.704$ ). The time necessary for a column to collapse is denoted as the critical time and designated as  $t_{cr}$  in table 1 and figures 4 and 5. Collapse always occurred suddenly. During the course of each test  $\Delta\epsilon_{av}$  was measured as a function of time in the manner previously described. The deflections due to load of a column can be expressed in terms of  $\Delta\epsilon(t)$  if it is assumed that cross sections of the column remain plane during bending and that the deflection  $w(t)$  is small and can be represented by a simple half-sine wave. Then

$$\Delta\epsilon(t) = h \left[ d^2w(t)/dx^2 \right] \quad (9)$$

$$w(t) = \bar{w}(t) \sin(\pi x/L) \quad (10)$$

and

$$\Delta\epsilon(t)_{av} = (3/2)(h/L) \int_{L/6}^{5L/6} \left[ d^2w(t)/dx^2 \right] dx \quad (11)$$

Hence

$$\bar{w}(t) = -(2/9\pi) \sqrt{3} \left( L^2/h \right) \Delta\epsilon(t)_{av} \quad (12)$$

in which  $\bar{w}(t)$  is the midpoint deflection at any time  $t$  and  $\Delta\epsilon(t)_{av}$  is the corresponding difference in the extreme fiber strains averaged over the central two-thirds of the column length. In figure 4 the ratio of the total midpoint deflection  $\bar{w}(t) + a_1$  to the column depth  $h$  is given as a function of the time. The value found for this ratio immediately prior to collapse is designated as  $w^*/h$  and is listed in table 1. It is seen to vary between 0.49 and 0.63 for this series of tests, and for a preliminary series of tests on columns of slenderness ratio 166 it ranged from 0.53 to 0.56. In reference 10 it was noted that for 7075-T6 aluminum-alloy columns having slenderness ratios of 30 to 100,

respectively, the quantity  $w^*/h$  varied from 0.10 to 0.75. These tests were performed at temperatures of 300 to 600° F. The small deflections encountered in reference 10 and in the present tests justify the use of equation (9), that is, a small-deflection theory.

The critical time  $t_{cr}$  given in table 1 is shown plotted against  $e_1$  in figure 5. The triangles and circles, respectively, correspond to values of  $e_1$  measured at room temperature and at test temperature for  $\alpha = 0.704$ . The remaining symbols represent data obtained from reference 11. The curves, which are based upon theory, will be discussed later. The results show that collapse time is much more sensitive to changes in end load than to changes in the initial deviation from straightness. As pointed out in reference 11, the results may also be influenced by the presence of higher harmonics in the initial deviation from straightness and by the preload required during the heating-up period. In addition, since 2024-T4 is a precipitation-hardened material, its physical properties may alter significantly with time at the test temperature of 600° F.

#### BENDING TESTS

In order to determine the material properties in creep bending of the 2024-T4 aluminum alloy of which the columns were fabricated, a series of pure-bending tests was performed at 600° F. Some of the geometrical and physical properties of the beams tested are:

Specimen size, in. . . . .	1/4 by 1/2 by 17
Test length, in. . . . .	12
Beam depth, h, in. . . . .	1/4
Modulus of elasticity at room temperature, E, psi . . . . .	$10.64 \times 10^6$
Modulus of elasticity at 600° F (see appendix), $E_T$ , psi . . . . .	$7.4 \times 10^6$

#### Test Apparatus and Procedure

The test apparatus consists of an oven capable of maintaining constant temperatures up to 1,000° F and a loading device designed to apply a pure bending moment to beams of rectangular cross section (figs. 6 and 7). It may be noted from figure 7 that the entire apparatus is supported on shock-absorbing shoes to reduce the transmission of vibrations to the test specimen.

Oven.- The oven consists of a bottom plate and a cover (fig. 7). To the bottom plate, which is fabricated from 1-inch-thick Transite, are

attached two 1,000-watt and two 250-watt electric strip heaters as well as knife-edge supports for the beam (fig. 6). The cover is made of two boxes of Transite plate with 3-inch-thick magnesia block insulation between the walls. The inner volume of the assembled oven is approximately 1/2 cubic foot. Thirty minutes at full power is required to obtain a temperature of 600° F, and one-third of this power is required to maintain this temperature during test.

Temperature measurement.- The temperature was measured along the 12-inch test length of the specimen with three equally spaced iron-constantan thermocouples which were connected through a switch to a Brown potentiometer (model 1117). The thermocouples were tied to the specimen with copper wire in such a manner that the hot junctions were in contact with the specimen. Since it was found that the temperature difference between any two stations was within 2° F, only the thermocouple at the middle of the specimen was used during the test. This thermocouple operated an automatic temperature controller (Phen-Trols) which maintained the test temperature to within ±3° F.

Curvature measurement.- Strain measurements were made in a manner analogous to that described previously. However, two gages were attached side by side to the upper face and to the lower face of the beam, each gage extending over the central one-third of the beam (fig. 6). The average strain difference so obtained is also the strain difference at any position along the beam because the beam under a pure bending moment deforms with a constant curvature change along its length and  $1/R = \Delta\epsilon/h$ , where R is the radius of curvature.

Test procedure.- The specimen was placed in position on the supporting knife edges, and, with the load supported by mechanical jacks, the loading knife edges were placed on the beam. The oven was then assembled and the temperature of the specimen stabilized at 600° F. Before the load was transmitted from the jacks to the beam, the strain-indicator reading was taken. A reading was also made shortly after the jacks were lowered. The time lapse between the first and second measurements was from 20 to 30 seconds. For the first several minutes after loading, readings were taken at the end of each minute; thereafter, intervals of  $2\frac{1}{2}$  to 5 minutes were used. The test was terminated before excessive deformations were obtained but not before 2 to 3 hours of steady creep was observed.

#### Results of Creep-Bending Tests

The results of four creep-bending tests are given in figure 8 and table 2. In figure 8 the curvature  $1/R$  is plotted against time. Since the time interval between loading and the first test point is not known accurately, all points in figure 8 are subject to a possible shift

equivalent to 20 to 30 seconds. The points shown along the axis of ordinates are computed from an elastic analysis with  $E_T = 7.4 \times 10^6$ . A considerable portion of each plot is seen to lie in a range of approximately steady creep rate of the curvature. A straight line drawn through the corresponding points of each of these plots yields the rates given in table 2. The corresponding intercepts are designated as  $1/R_0$ . The curvatures calculated from elastic analysis are designated as  $1/R_e$ .

If the steady creep rate  $d(1/R)/dt$  from table 2 is plotted on a logarithmic scale as shown in figure 9, a straight line can be drawn through the plotted points. Thus, the creep rate can be represented by a power law of the form

$$d(1/R)/dt = kM^m \quad (13)$$

in which  $M$  is the applied moment and  $k$  and  $m$  are constants. With the data given in table 2, the method of least squares yields  $m = 2.94$  and  $k = 808 \times 10^{-12}$ . If  $m$  is taken as the nearest integer,

$$m = 3 \quad (13a)$$

and  $k$  becomes

$$k = 633 \times 10^{-12} \text{ in.}^{-4} \text{ lb}^{-3} \text{ min}^{-1} \quad (13b)$$

These values are used in the analysis. When inserted into equation (13), they yields values of the creep rate in very good agreement with the experimental values (compare the third and last columns of table 2).

#### CORRELATION OF THEORY AND EXPERIMENT FOR CREEP BUCKLING

An analysis of creep-bending and creep buckling of an idealized H-section beam column was presented in references 5 and 6. In this work a power-function creep law was assumed in the form

$$d\epsilon/dt = (1/E_1)(d\sigma/dt) + (\sigma^m/\lambda) \quad (14)$$

in which  $\epsilon$  is the creep strain,  $\sigma$  is the stress, and  $E_1$ ,  $\lambda$ , and  $m$  are creep constants. The analysis presented could be extended in the manner of Libove (ref. 2) to columns of rectangular cross section, but

the amount of labor required for the calculations does not appear justified, particularly in view of the many simplifying assumptions necessary. Instead, the simple closed-form results of references 5 and 6 are used in conjunction with an effective H-section depth defined so that the static properties of the rectangular and idealized H section are equivalent. Thus, since the moment of inertia  $I$  and area  $A$  of the equivalent H section, respectively, must equal the moment of inertia and area of the rectangular section, the equivalent depth is

$$h^* = h/\sqrt{3} \quad (15)$$

In the case of pure bending of a beam whose creep parameters are the same in tension or compression, equation (12) of reference 5 yields

$$d(1/R)/dt = (2/\lambda h^*)(2M/Ah^*)^m \quad (16)$$

When applied to the H-section equivalent of the rectangular section, equation (16) together with equation (15) yields

$$d(1/R)/dt = \left(2\sqrt{3}/\lambda h\right) \left(2\sqrt{3}M/Ah\right)^m \quad (17)$$

This equation is seen to be of the same form as the empirically derived equation (13).

The corresponding creep deflection-time characteristics of a simply supported column can be obtained from reference 5 or 6. It is hypothesized in these references that the creep constants involved can be determined from simple uniaxial creep tests together with equation (14). The actual loading of a column involves both simple axial compression and bending. Because of the importance of the bending, it is probably more justifiable to obtain the creep constants from creep-bending tests than from uniaxial creep tests. Hence, for the present analysis the creep constants  $m$  and  $\lambda$  are determined with the aid of equation (17) and the results of the pure-bending tests. The creep constant  $m$  of equation (17) is then equal to the corresponding experimentally determined value in equation (13), and the creep constant  $\lambda$  is related to  $k$  according to

$$\lambda = \left(2\sqrt{3}/kh\right) \left(2\sqrt{3}/Ah\right)^m \quad (18)$$

From equations (13a) and (13b),  $m = 3$  and  $k = 633 \times 10^{-12} \text{ in.}^{-4} \text{ lb}^{-3} \text{ min}^{-1}$ , and, from the specimen properties given previously,  $h = 1/4$  inch and  $A = 1/8$  square inch. Hence, equation (18) yields

$$\lambda = 298 \times 10^{14} \text{ in.}^{-6} \text{ lb}^3 \text{ min} \quad (18a)$$

In reference 6 closed-form expressions are given for the creep deflection-time characteristics of H-section columns for arbitrary integral values of  $m$ . For the case  $m = 3$ , table 2 of reference 5 yields

$$z = f_{T_0} \left\{ 3e^{3\tau} / \left[ 4f_{T_0}^2 (1 - e^{3\tau}) + 3 \right] \right\}^{1/2} \quad (19)$$

and

$$\tau_{cr} = (1/3) \log_e \left[ 1 + \left( 3/4f_{T_0}^2 \right) \right] \quad (20)$$

in which  $z$  and  $f_{T_0}$ , respectively, are the ratios of the total midpoint deflection to the column depth at any time  $t$  and immediately after loading (at  $t = 0$ ),  $\tau$  is a nondimensional time parameter, and  $\tau_{cr}$  is the corresponding critical-time parameter. In the notation of the present report

$$f_{T_0} = (a_1/h^*) / \left[ 1 - (\bar{\sigma}/\sigma_E) \right] \quad (21a)$$

$$z = (1/h^*) \left[ \bar{w}(t) + a_1 \right] \quad (21b)$$

$$\tau = 2(E_1/\lambda) \left[ \bar{\sigma}^3 / (\sigma_E - \bar{\sigma}) \right] t \quad (21c)$$

$$\bar{\sigma} = P/A \quad (21d)$$

$$\sigma_E = (\pi\rho/L)^2 E_1 \quad (21e)$$

In equations (14), (21c), and (21e) the constant  $E_1$  appears. It is seen from reference 5, or directly from equation (14), that  $E_1$  is an effective modulus corresponding to the intercept of the creep-strain axis of the straight line obtained in a plot of  $\epsilon$  versus  $t$  for constant stress. Since the value of this strain intercept is always greater than the corresponding elastic strain, the effective modulus  $E_1$  is always less than the actual elastic modulus. Hence, if equation (21e) were used, the Euler stress so obtained would be less than the actual instantaneous buckling stress; and particularly when the applied stress  $\bar{\sigma}$  is close to the actual buckling stress, equations (21a) and (21c) would

yield unrealistic (negative) values. In view of this,  $E_1$  is taken as the actual elastic modulus at test temperature given earlier as  $E_T = 7.4 \times 10^6$  psi. Values for  $E_1$  determined from the bending tests and the relation  $1/R_0 = M/E_1 I$  are given in table 2.

The critical time obtained from equation (20) with  $E_1 = E_T$  is plotted in figure 5. In general, the calculated results are in poor agreement with the test results, particularly in the region of large initial deviation from straightness. In the theory this critical time corresponds to infinite deflections and, hence, in part, to a region in which the deflections are too large to be accurately characterized by the small-deflection theory employed. Rather, useful column life might be characterized by a limiting deflection, small enough so that the results of the theory employed can be justified at least in this respect. The curves of deflections versus time given in reference 5 indicate that, after the total midpoint deflection of the column becomes equal to half the depth of the column (i.e.,  $z = 1/2$ ), the deflections increase very rapidly. At this time the stress in the convex flange of the H section is zero and thereafter becomes tensile. Of course, the corresponding action of a solid-section column would not be so drastic, since stress reversal starts only at the extreme fiber of the convex side. The test data for the present series of column tests also indicate that column collapse starts when  $w^*/h$  is approximately  $1/2$ . However, the data given in reference 10 and mentioned earlier show that  $w^*/h$  ranges from 0.10 for slenderness ratios of 30 to 0.75 for slenderness ratios of 100 for a wide range of column parameters for 7075-T6 aluminum alloy. This, of course, suggests that choosing  $z = 1/2$  to determine an approximate value of the critical time is rather arbitrary. Nevertheless, when  $z$  is taken equal to  $1/2$  in equation (19) and the remaining parameters are chosen as described previously, the solid curves shown in figure 5 are obtained. These curves depict the trend of the data fairly well. The corresponding equation in terms of the parameter  $\tau_1$ , which corresponds to the time at which  $z = 1/2$ , is from equation (19):

$$\tau_1 = (1/3) \log_e \left\{ (1/4) \left[ 1 + (3/4) \left( 1/\rho_{T_0} \right)^2 \right] \right\} \quad (22)$$

From equations (21c) and (22), the time  $t_1$  is

$$t_1 = (1/6) (\lambda/E_1) (1/\bar{\sigma})^2 \left[ (1/\alpha) - 1 \right] \log_e \left\{ (1/4) \left[ 1 + (3/4) \left( 1/\rho_{T_0} \right)^2 \right] \right\} \quad (23)$$

It should be noted that when equation (22) or (23) is used  $E_1$  should be taken equal to  $E_T$ .

The experimental and semiempirical results shown in figure 5 are replotted in terms of the parameters  $\tau$  and  $f_{T_0}$  in figure 10. The scatter shown by the data is considerable. This is due in part to the experiments, the results of which were discussed previously (see fig. 5), and in part to the highly simplified form of the analysis employed. The results suggest, however, that, for columns whose slenderness ratios are of the order of those tested (111), equation (23) affords a reasonable guide for the estimation of the collapse time. The present work also indicates that, if a column is fabricated from a material whose behavior in creep bending can be characterized at the working temperature by a simple power function (eq. (13)), a semiempirical formula, corresponding to the appropriate value of the creep parameter  $m$ , can be obtained with the aid of reference 5 or 6 for estimating the critical time.

#### CONCLUDING REMARKS

The results of the present and previous creep-buckling tests on 2024-T4 aluminum-alloy columns of rectangular cross section indicate that the collapse or critical time decreases much more drastically with an increase in load than it does with a corresponding percentage increase in the amplitude of the initial deviation from straightness.

From creep-bending tests on 2024-T4 aluminum-alloy beams, it is concluded that the steady creep rate of the curvature is a simple power function of the applied bending moment. The creep constants determined with such a function are used in the correlation of the results of the column tests with those of a previously developed creep-buckling theory. This theory, which was derived for idealized H-section columns, is modified by the introduction of an H-section equivalent of the rectangular section, and a semiempirical formula based on the concept of a limiting deflection is suggested as a guide in determining collapse time.

Polytechnic Institute of Brooklyn,  
Brooklyn, N. Y., April 7, 1955.

## APPENDIX

## DEVELOPMENT OF HIGH-TEMPERATURE STRAIN GAGE

In the investigation of creep buckling it appeared desirable to measure changes in strain in columns at elevated temperatures over extended periods of time. As commercially available strain gages were not suitable for this purpose, an electric-resistance strain gage was developed as part of the investigation. In its present form the strain gage is a single straight Cupron wire bonded to the specimen in which the strain is to be measured. The end sections of the gage are copper plated; these sections replace the lead wires which in the commercially available gages are thicker wires welded to the thinner gage wire. The copper-plating procedure is also useful in controlling the effective gage length. Details of the manufacturing process are given, and tests are described which indicate proper functioning of the gages at a temperature of 600° F.

## DESCRIPTION OF STRAIN GAGE AND OF

## ITS MANUFACTURING PROCESS

## Choice of Wire

As the strain gage is to measure strains at various temperatures, the wire chosen for it should function properly at elevated temperatures and it should have as small a change in resistance with temperature as possible. The material selected is Cupron wire manufactured by the Wilbur B. Driver Co. of Newark, N. J. The diameter of the wire is 0.001 inch and its resistance, 281 ohms per foot.

## Copper Plating of Ends of Gage

The ends of the gage are copper plated for a number of reasons. First, the process used for copper plating allows a control of the effective gage length with satisfactory accuracy. Secondly, the thickened ends of the wire are sturdy, make possible the handling of the unattached gage without extreme care, and eliminate a great deal of breakage such as occurred in the neighborhood of the welded joints at the ends of the earlier gages. In consequence of the plating it is not necessary to weld thicker lead wires to the thin gage wire proper; the thickened sections serve as lead wires and allow easy attachment to the wires of the electric circuit. Finally, the welds of the earlier gages are known to have

caused irregularities in the resistance of the gages when the temperature changed; this effect is eliminated when welding is abandoned.

The plating is done in an acid tank with an electrolyte containing the following chemicals per gallon of solution:

CuSO <sub>4</sub> ·5H <sub>2</sub> O, oz . . . . .	24
H <sub>2</sub> SO <sub>4</sub> , oz . . . . .	6

In addition, a mucilage glue is used as a brightener; 1/8 ounce of it is added to each gallon of the solution. The tank is a glass container of 5- by 10-inch base and 7 inches in height; 1/6-inch-thick copper plates placed in it serve as the anode.

Many gages are plated simultaneously by partially submerging a long wire and cutting it into shorter elements after completion of the copper plating. Each gage wire is wound about 20 times around a rectangular frame of stainless steel. Three such frames are connected in parallel and form the cathode; they slide in the grooves of two vertical blocks of lucite mounted on a metal base, and the assembly is placed in the acid tank. The blocks and the frames with plated wires are shown in figure 11 and the assembly in the glass tank, together with the electric power supply, can be seen in figure 12.

The length of the gage is controlled by adjusting the level of the electrolyte. The total unsubmerged length of each turn of the wire on the frame is the gage length, and the two copper-plated ends of the same turn can be considered the lead wires. Gages made with the same level of the electrolyte naturally have the same length.

It was found advantageous to increase the diameter of the wire in two steps. In the first operation the diameter is allowed to increase to about 0.012 inch. Then the level of the electrolyte is lowered 3/8 inch or 1/2 inch and the plating process is continued until the final diameter is approximately 0.025 inch. The two-step arrangement results in a satisfactory attachment of the gage to the specimen as is illustrated in figure 13. After it is annealed, the 0.025-inch-thick wire has good resistance to bending and twisting and does not break easily when it is connected to the wires of the electric measuring circuit.

In the power supply of the copper-plating process a filament transformer reduces the 110- to 115-volt alternating current to 10 volts of alternating current. The reduced-voltage current enters a selenium rectifier to obtain a direct current. Capacitors are used on the direct-current side of the circuit to diminish fluctuations in the voltage. In the plating process described the maximum voltage of the direct current was 8 volts and the maximum current, 18 amperes.

The circuit diagram is presented in figure 14 in which the components shown are specified as follows:

- T<sub>1</sub>            Variac (controls voltage supply to primary of the transformers):  
                 0 to 135 volts alternating current, 700 watts
- T<sub>2</sub>, T<sub>3</sub>       filament transformers: Triod F-11-U
- V              selenium rectifier: Sarkes Tarzian, catalog no. D-16
- C              two capacitors: Mallory metal can electrolytic, catalog  
                 no. W.P. 041

#### Annealing of Gages

When wire strain gages are used for prolonged periods of time at high temperatures, they are likely to oxidize with a consequent change in their electric resistance. To insure that the gage will yield stable readings, that is, that the readings on an instrument will not vary with time when the strain is kept constant, it is advantageous to preoxidize the wire. This can be accomplished by heating the wire to a sufficiently high temperature and by maintaining it at that temperature long enough during the manufacturing process. The heating has the added advantage that it anneals the copper deposit and increases its ductility.

Of course, heat treatment may influence the Cupron gage wire also, which is objectionable. As the annealing temperature of the gage wire is about 1,200° F, the gage should be annealed below 1,200° F. On the other hand, the gage must be heated above 600° F because the annealing temperature of the copper plating is between 600° and 1,200° F. Finally, the heat treatment must be undertaken at a temperature well above the temperature at which the strain gages will be used because, otherwise, the layer of oxide may increase in thickness during the test. A series of experiments has shown that the best results are obtained when the gages are annealed at 800° F for 1 hour.

The actual annealing process is carried out in the following manner: After completion of the copper plating the wires are cut along the bottom edge of the stainless-steel frame. The individual gages so obtained are straightened out and are placed loosely, without being stretched, on an aluminum plate. The ends of the lead wire are attached to the plate by means of drafting tape (Minnesota Mining and Manufacturing Co.), and the plate is placed horizontally in an oven. The oven is heated to 800° F and maintained at that temperature for 1 hour. At the end of the heating period the gages are allowed to cool slowly to room temperature. They are removed from the oven with care because the drafting tape is charred and does not hold them to the plate. The individual gages are placed

on sheets of paper to which they are attached by adhesive tape applied to the thickened ends; they are then ready for use.

#### ATTACHMENT OF STRAIN GAGE TO SPECIMEN

The strain gage must be bonded to the test specimen in which the strain is to be measured. Before attachment, the surface of the specimen must be prepared in the following manner:

- (1) The surface is cleaned with emery paper and acetone in the standard manner.
- (2) A thin layer of Dow-Corning varnish no. 993 is applied with an artist's brush.
- (3) The varnish is cured as directed by the manufacturer.
- (4) The shine is removed with emery paper.
- (5) The procedure described under items (2) to (4) is repeated.

When the preparation of the surface is completed, the strain gage is attached in the following steps:

- (1) The strain gage is placed on the surface of the specimen. Care must be exercised to keep the gage straight without any tension.
- (2) To maintain the gage in the desired location and to keep it in contact with surface of the specimen, the thickened ends of the wire are attached to the specimen by means of drafting tape. The tape has been found to work satisfactorily up to temperatures of 650° to 700° F.
- (3) A thin layer of Dow-Corning varnish no. 993 is applied with an artist's brush.
- (4) The varnish is cured as directed by the manufacturer.
- (5) The procedure described under items (3) and (4) is repeated.

The strain gage is then bonded to the test specimen; its ends can be connected with the wires of the electric measuring circuit.

## EXPERIMENTS

A few experiments have been carried out to verify the proper functioning of the high-temperature strain gages. In one test, readings of this strain gage were compared with readings of standard Baldwin-Southwark SR-4 strain gages; all the gages were attached to a beam subjected to a constant bending moment at room temperature. This test yielded a gage factor of 2.1 for the high-temperature strain gage, and the same value was obtained at 600° F.

Other tests were carried out with a column of a series used for preliminary tests in creep buckling. The column was placed in an oven and the load was applied to it by means of a lever with an advantage of 5 to 1. Simultaneous readings were made of the load and of the average change in resistance in the strain gages bonded to opposite sides of the column, and the latter values were converted into average strain with the aid of the gage factor of 2.1. The stress-strain curves derived from these data are shown in figure 15. One of the two tests represented in the figure was carried out at a temperature of 72° F and the other, at 600° F. The curves are straight lines; their slopes are proportional to Young's modulus of the material. At room temperature the value of  $10.64 \times 10^6$  psi was obtained for the modulus. At 600° F the corresponding value was  $7.40 \times 10^6$  psi. The test at 600° F was carried out at the highest possible speed to avoid creep deformations.

The column was 12 inches long and had a cross section of 1/2 by 1/4 inch; its material was 2024-T4 aluminum alloy. It had a slenderness ratio of 166.2; consequently, it was easy to determine its buckling load experimentally at room temperature without causing permanent deformations. The critical strain of a perfectly elastic column is  $(\pi r/L)^2$  and, hence, the theoretical critical strain of the column tested was  $356 \times 10^{-6}$ . At 0.988 times the critical load the theoretical strain was  $352 \times 10^{-6}$ ; the experimental strain was found to be  $351 \times 10^{-6}$ .

If the column also behaves perfectly elastically in the test at 600° F, the theoretical critical strain is unchanged even though the modulus is reduced. At 0.991 times the critical load corresponding to the high temperature, theory yielded a strain of  $353 \times 10^{-6}$  and experiment, one of  $350 \times 10^{-6}$ .

It can be concluded that the high-temperature strain gage developed adhered well to the surface of aluminum-alloy specimens and appeared to be stable at a temperature of 600° F.

## REFERENCES

1. Libove, Charles: Creep Buckling of Columns. Jour. Aero. Sci., vol. 19, no. 7, July 1952, pp. 459-467.
2. Libove, Charles: Creep-Buckling Analysis of Rectangular-Section Columns. NACA TN 2956, 1953.
3. Hilton, Harry H.: Creep Collapse of Viscoelastic Columns With Initial Curvatures. Jour. Aero. Sci., vol. 19, no. 12, Dec. 1952, pp. 844-846.
4. Higgins, T. P., Jr.: Effect of Creep on Column Deflection. Pt. III, Ch. 20 of "Weight-Strength Analysis of Aircraft Structures" by F. R. Shanley, First ed., McGraw-Hill Book Co., Inc., 1952, pp. 359-385.
5. Kempner, Joseph: Creep Bending and Buckling of Nonlinearly Viscoelastic Columns. NACA TN 3137, 1954; see also PIBAL Rep. No. 200, May 1952.
6. Kempner, Joseph, and Patel, Sharad A.: Creep Buckling of Columns. NACA TN 3138, 1954; see also PIBAL Rep. No. 205, Nov. 1952.
7. Jackson, L. R., Schwope, A. D., and Shober, F. R.: Stress-Strain-Time Properties of Some Aircraft Materials. Pt. III, Ch. 17 of "Weight-Strength Analysis of Aircraft Structures" by F. R. Shanley, First ed., McGraw-Hill Book Co., Inc., 1952, pp. 307-322.
8. Rosenthal, D., and Baer, H. W.: An Elementary Theory of Creep Buckling of Columns. Proc. First U. S. Nat. Cong. Appl. Mech. (June 1951, Chicago, Ill.), A.S.M.E., 1952, pp. 603-611.
9. Carlson, R. L., and Schwope, A. D.: An Experimental Investigation of Creep Properties of Aluminum at Elevated Temperatures. Proc. First Midwestern Conf. Solid. Mech., Eng. Exp. Station, Univ. of Ill., Apr. 1953, pp. 180-183.
10. Mathauser, Eldon E., and Brooks, William A., Jr.: An Investigation of the Creep Lifetime of 75S-T6 Aluminum-Alloy Columns. NACA TN 3204, 1954.
11. Patel, Sharad A., Bloom, Martin, Erickson, Burton, Chwick, Alexander, and Hoff, N. J.: Development of Equipment and of Experimental Techniques for Column Creep Tests. NACA TN 3493, 1955; see also PIBAL Rep. No. 239, Dec. 1953.

TABLE 1.- RESULTS OF COLUMN TESTS

Column	$\epsilon_E$	$e_1$	$e_{1hot}$	$t_{cr}$ , min	$w^*/h$
1	$828 \times 10^{-6}$	0.045	0.035	80.95	0.496
2	842	.075	.084	54.00	.492
3	845	.096	.072	28.30	.560
4	820	.111	.093	26.05	.526
5	879	.168	.123	32.00	.634
6	820	.184	.131	18.88	.562
Calculated	801	-----	-----	-----	-----

TABLE 2.- RESULTS OF BENDING TESTS AND CALCULATIONS

Beam	Applied moment, M lb-in.	Steady creep rate, $\frac{d}{dt}\left(\frac{1}{R}\right)$ , in. <sup>-1</sup> min <sup>-1</sup>	Intercept, 1/R <sub>0</sub> , in. <sup>-1</sup>	Elastic curvature, 1/R <sub>e</sub> , in. <sup>-1</sup>	E <sub>1</sub> , psi	$\left[\frac{d}{dt}\left(\frac{1}{R}\right)\right]_{\text{calc}}$ , in. <sup>-1</sup> min <sup>-1</sup>
1	40.00	$42 \times 10^{-6}$	$15.8 \times 10^{-3}$	$8.3 \times 10^{-3}$	$3.9 \times 10^6$	$41 \times 10^{-6}$
2	54.85	102	17.7	11.4	4.8	107
3	60.00	131	14.9	12.5	6.2	137
4	64.85	180	18.1	13.5	5.5	173

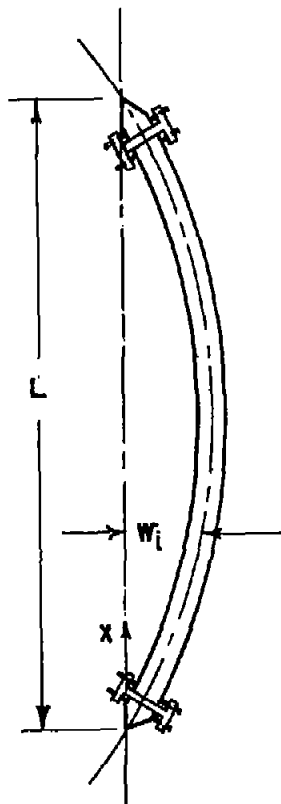
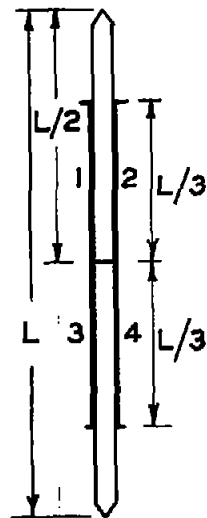
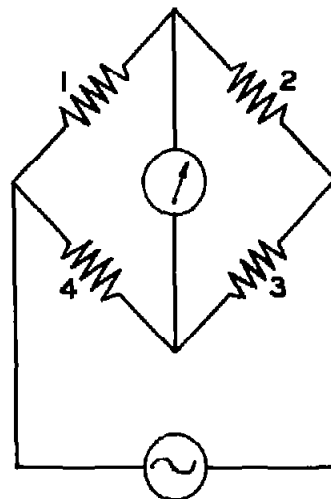


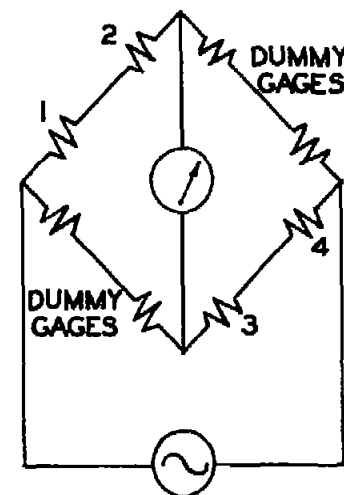
Figure 1.- Coordinate system for simply supported beam.



(a) Location of gages on specimen.



(b) Bridge formed by connecting gages to strain indicator.



(c) Switching system coupling gages.

Figure 2.- Gage locations and bridge circuits.

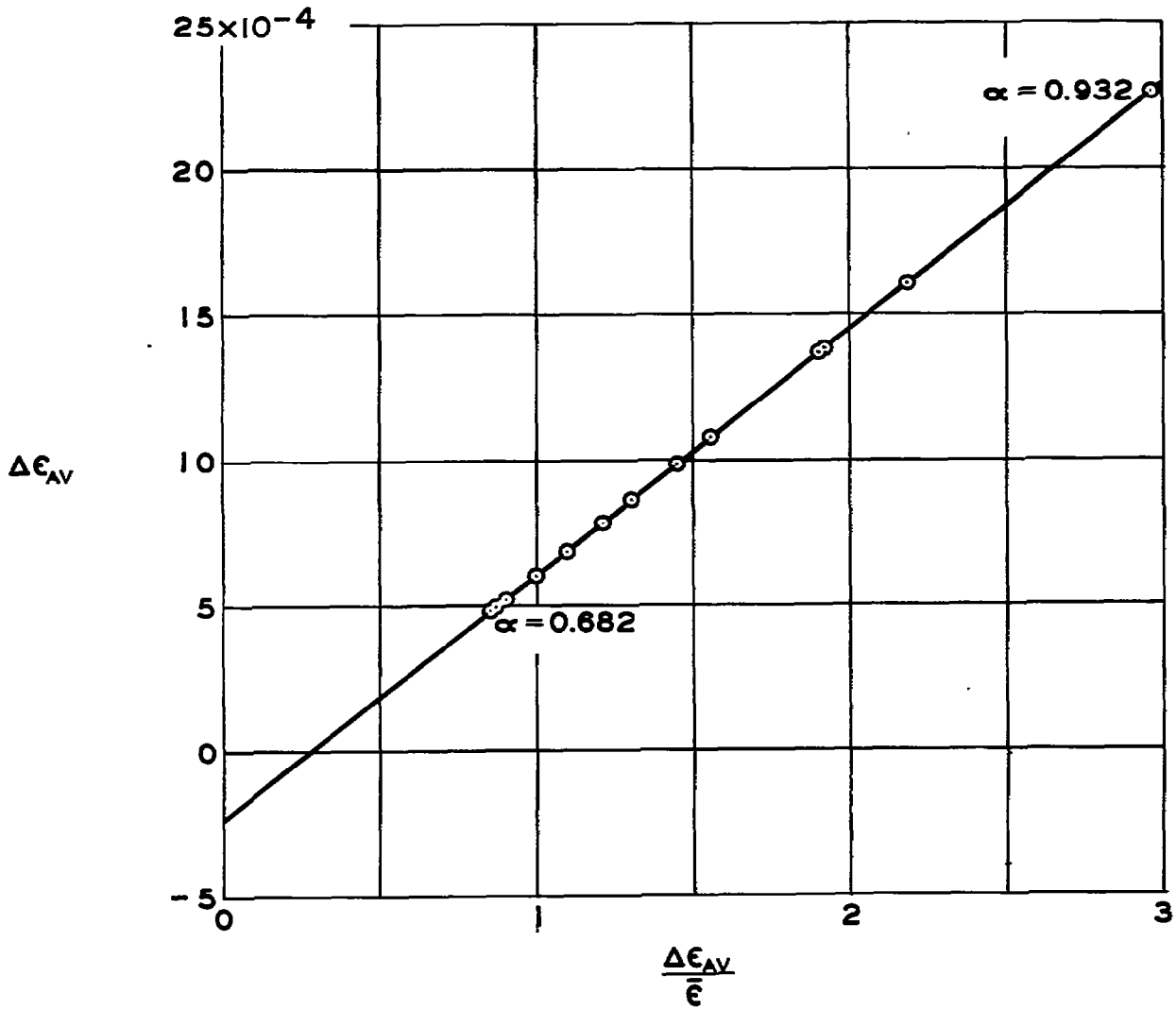
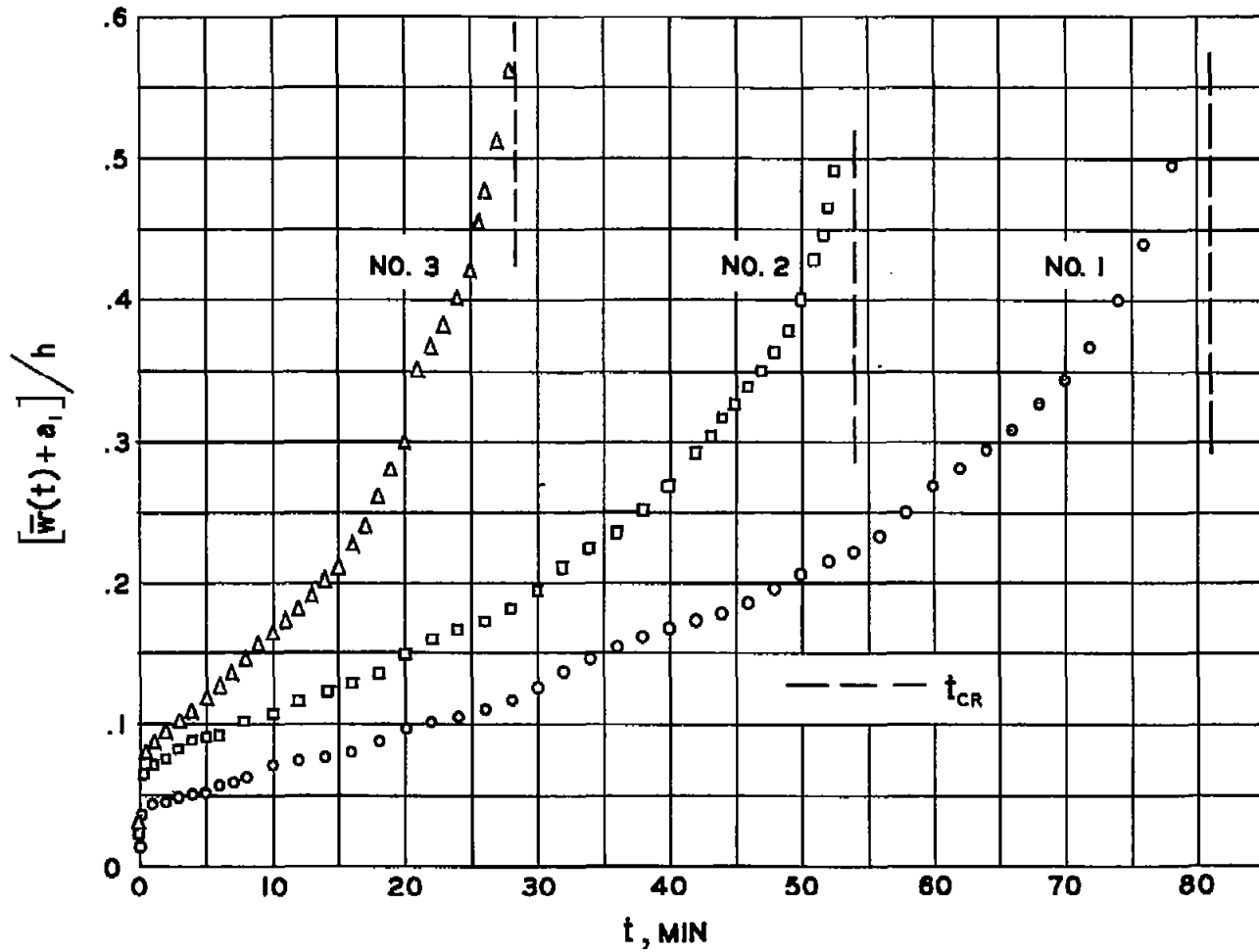
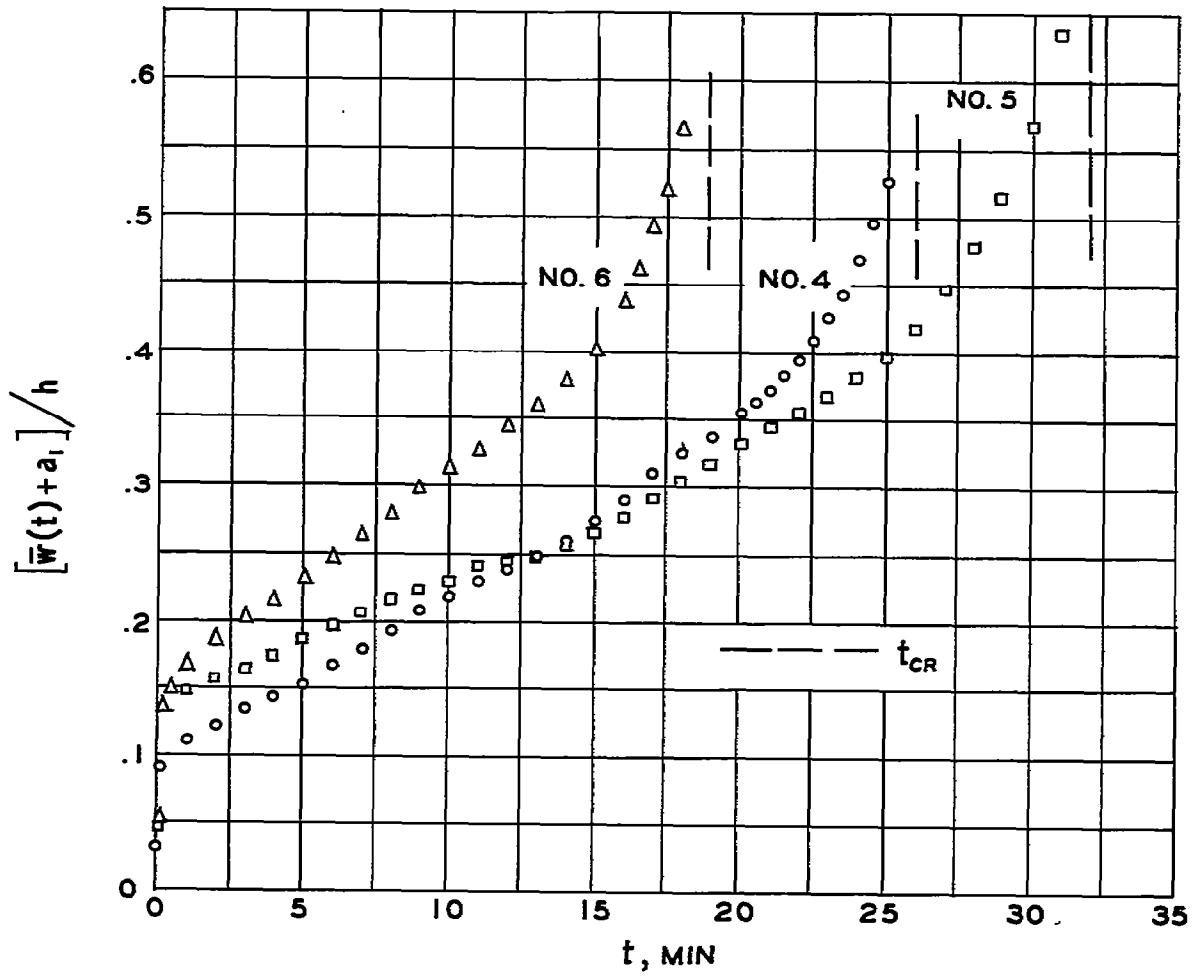


Figure 3.- Plot used in determination of  $\epsilon_E$  and  $e_1$ . Column 3;  
 $\epsilon_E = 845 \times 10^{-6}$ ;  $e_1 = 0.096$ .



(a) Columns 1 to 3.

Figure 4.- Variation of midpoint deflection of column with time  
 $(\alpha = 0.704)$ .



(b) Columns 4 to 6.

Figure 4.- Concluded.

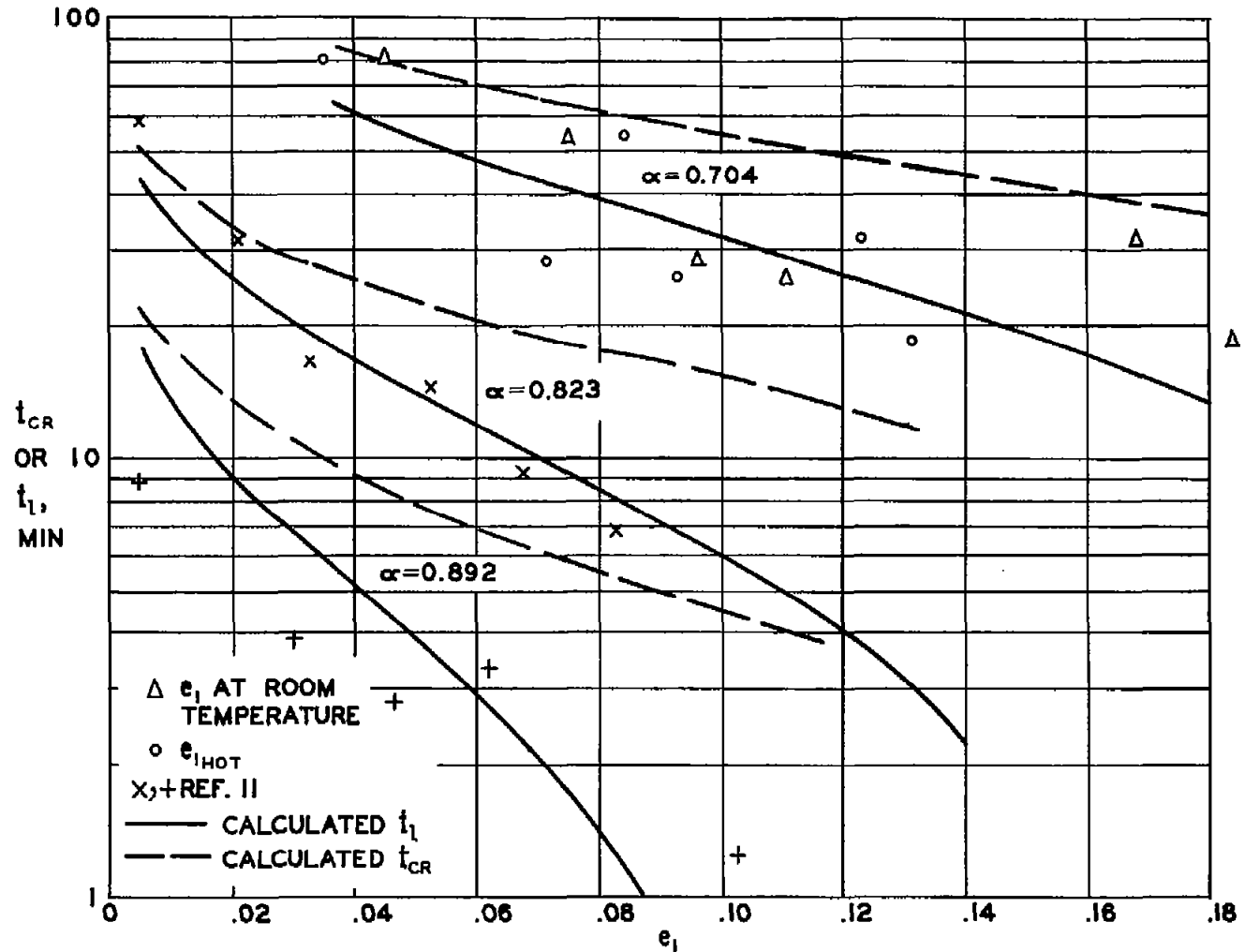


Figure 5.- Variation of critical time with initial deviation from straightness.

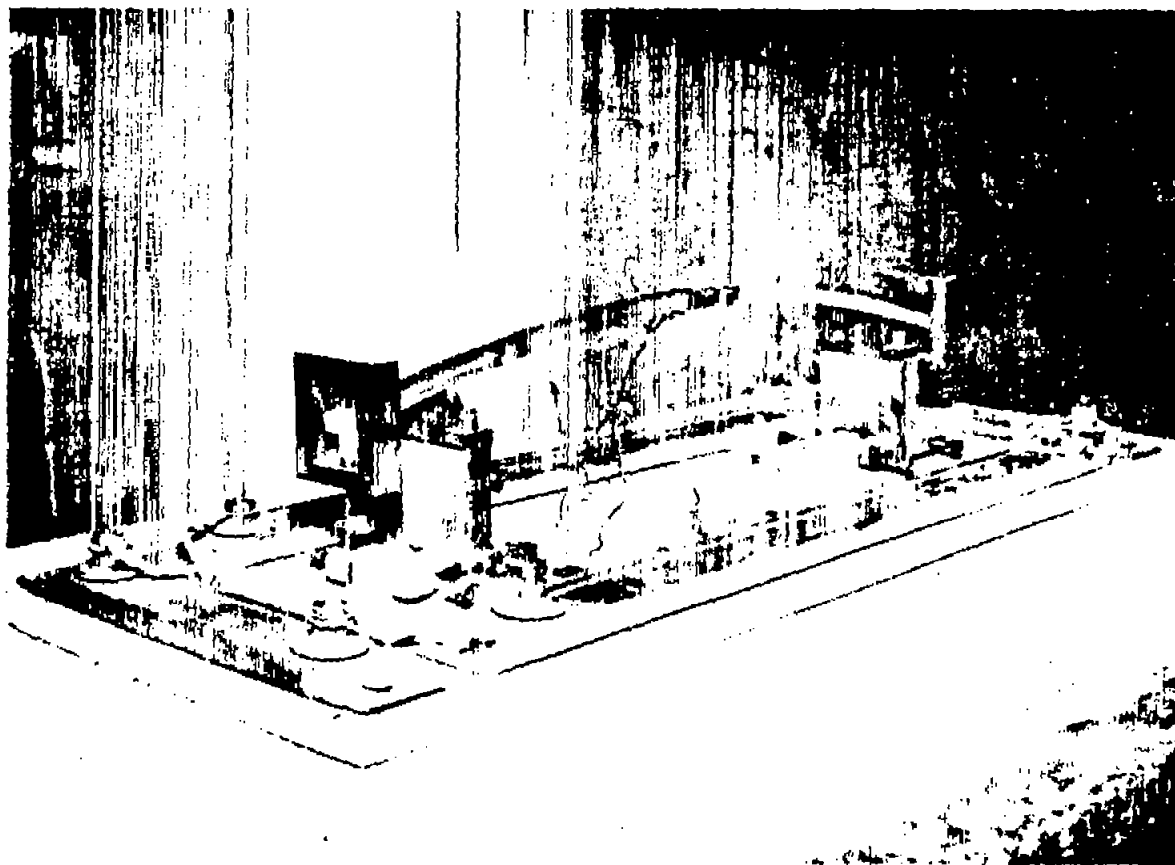


Figure 6.- Bending specimen and bottom plate of oven. L-92484

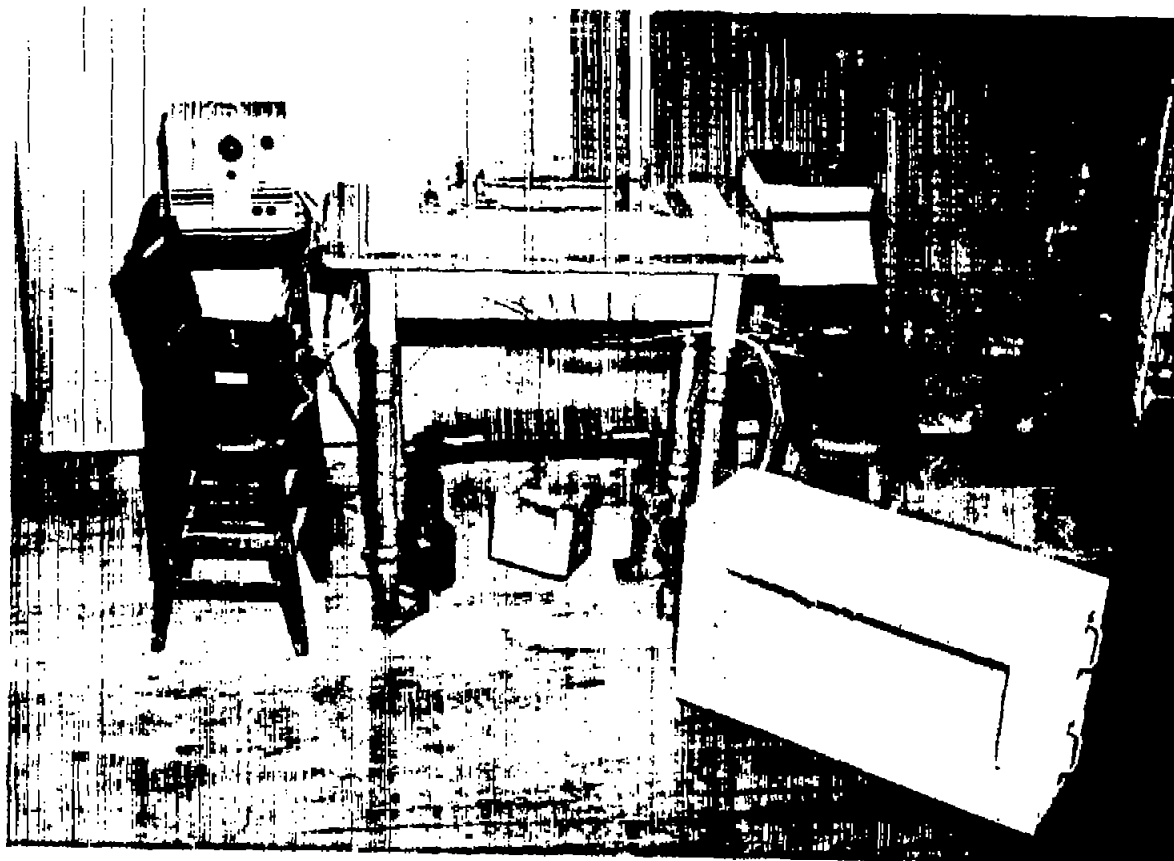


Figure 7.- Bending test setup.

L-92485

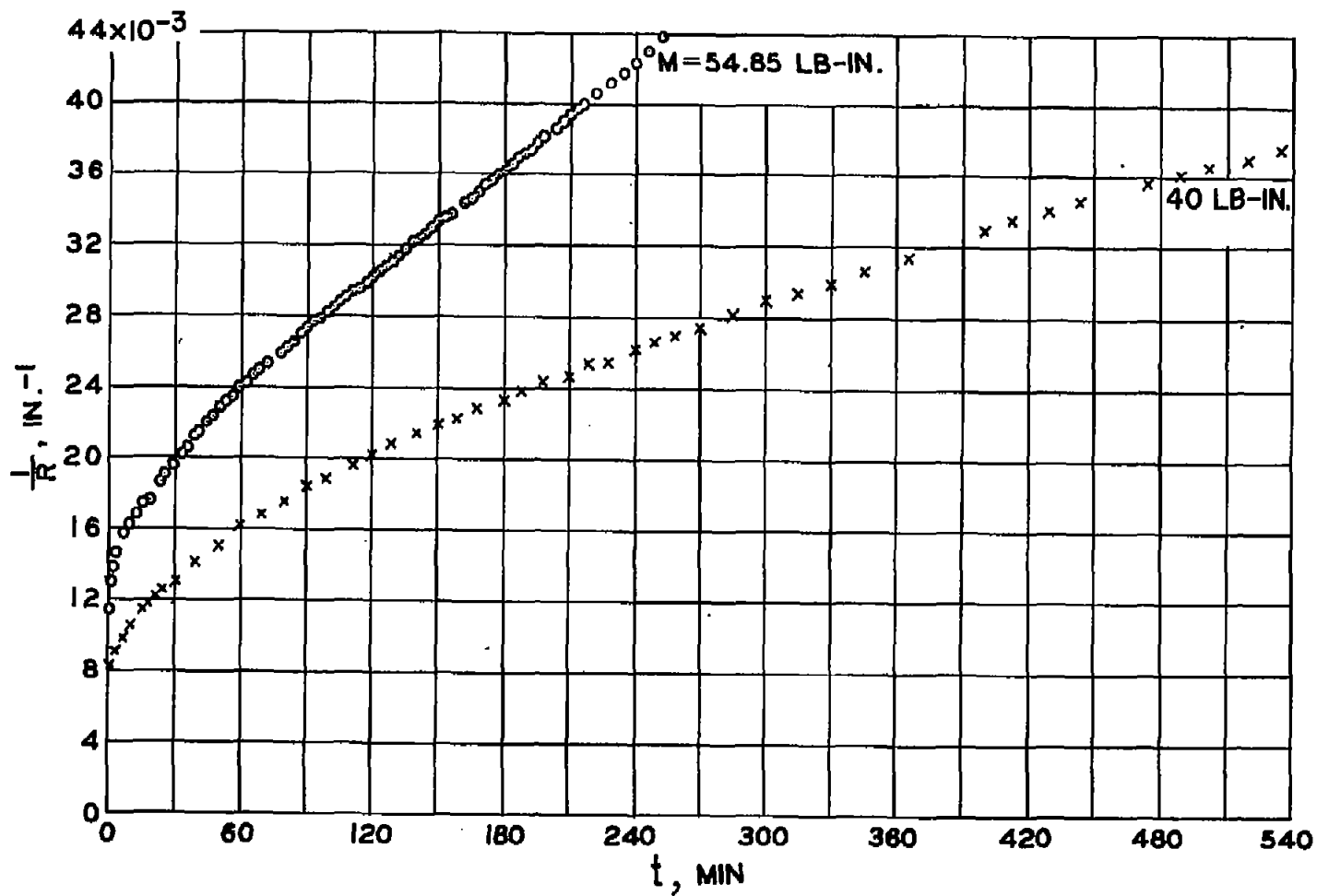
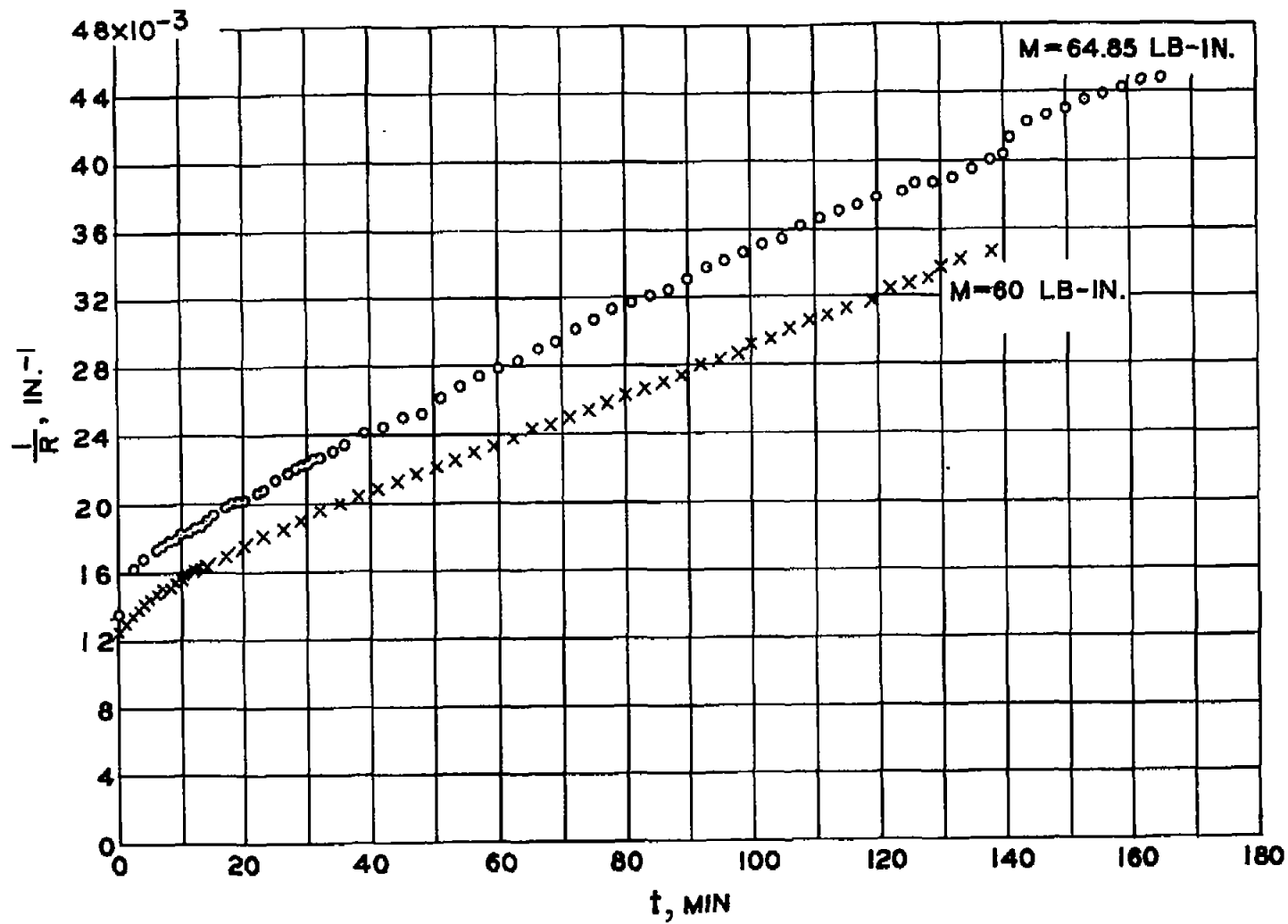
(a)  $M = 40$  and  $54.85$  lb-in.

Figure 8.- Variation of curvature with time for pure bending.



(b)  $M = 60$  and  $64.85$  lb-in.

Figure 8.- Concluded.

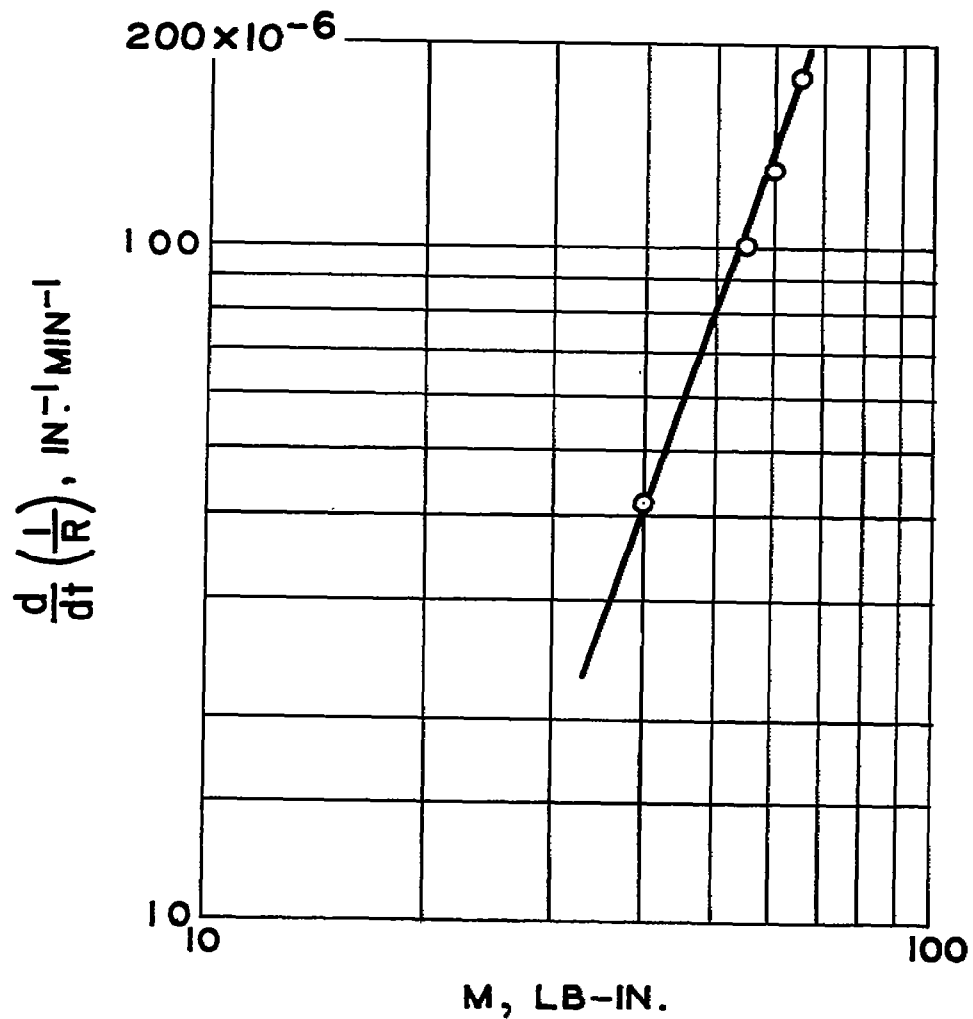


Figure 9.- Variation of steady creep rate of curvature with bending moment.

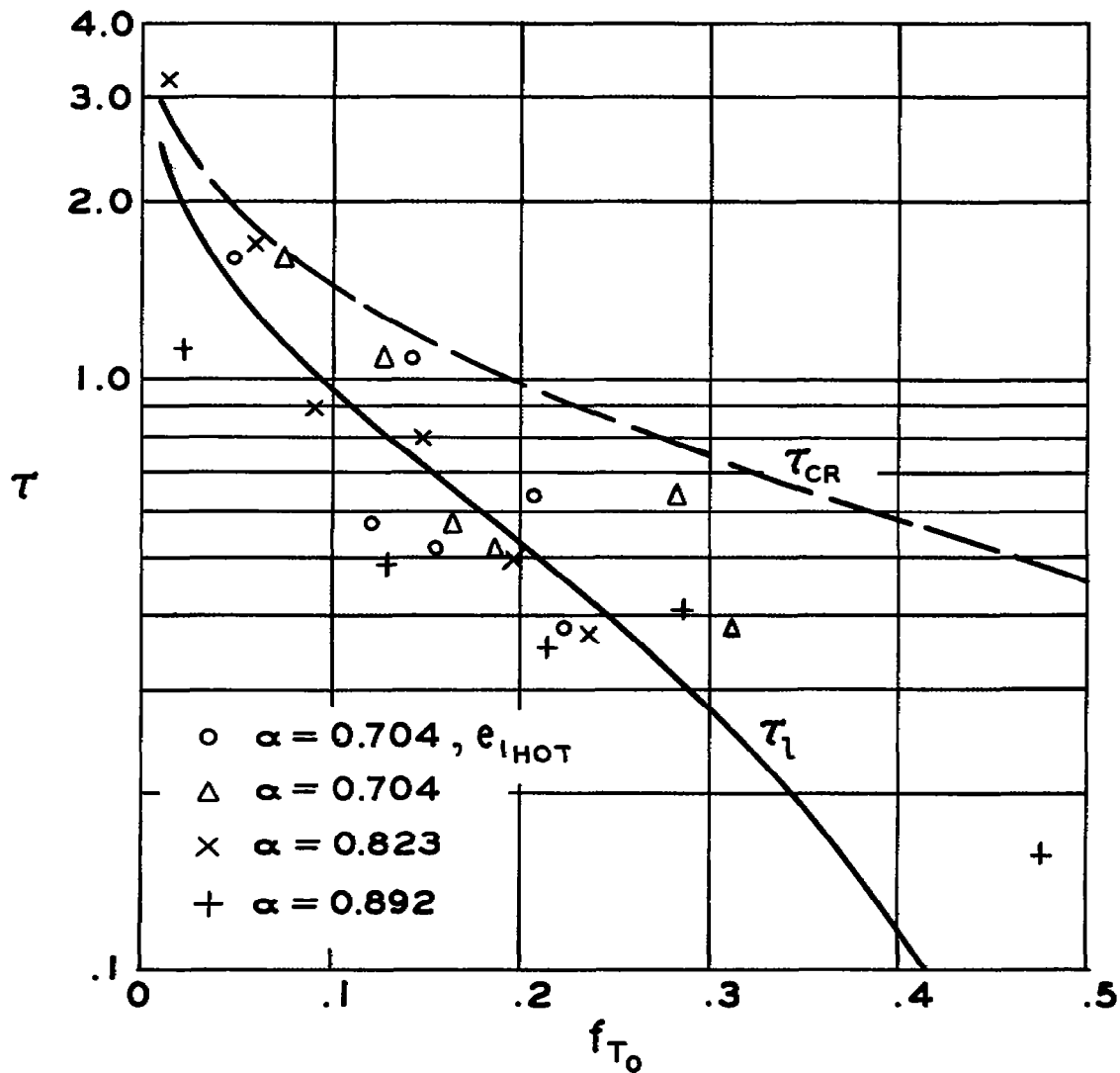


Figure 10.- Variation of experimental and calculated critical-time parameters with  $f_{T_0}$ .

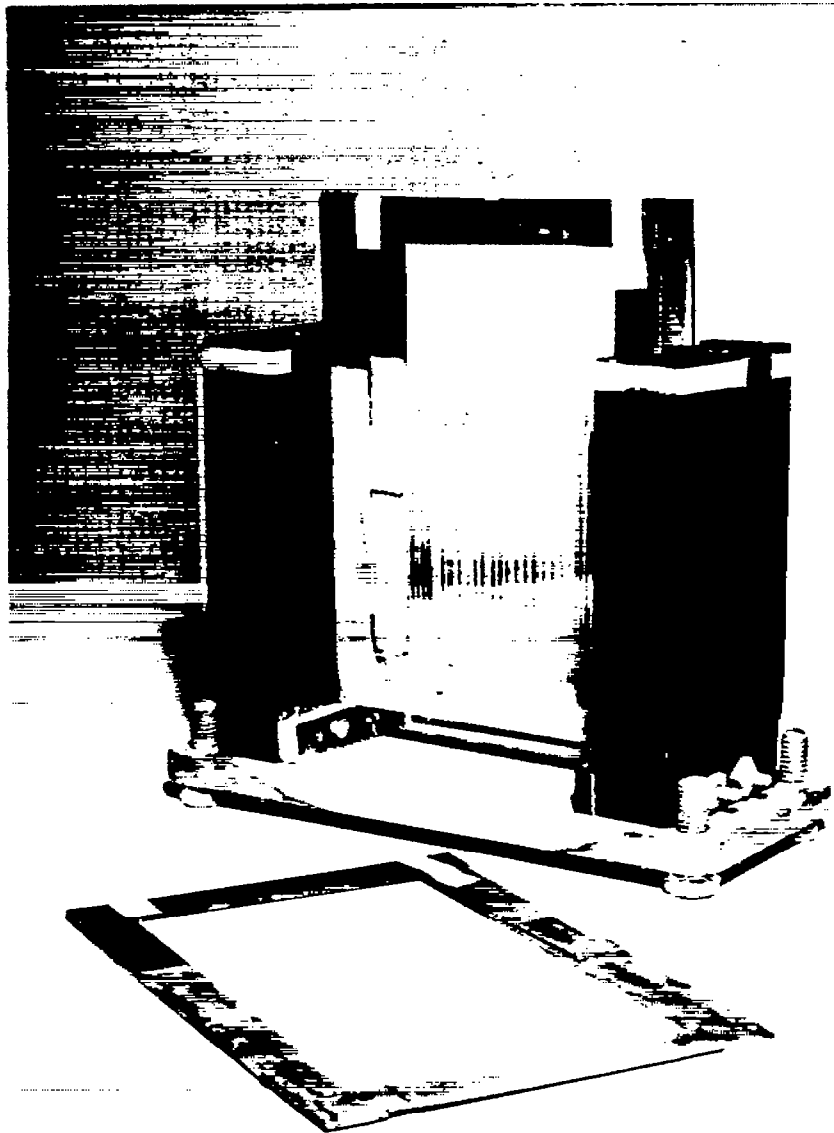


Figure 11.- Winding frames and holder for copper plating gage lead wires. L-92486

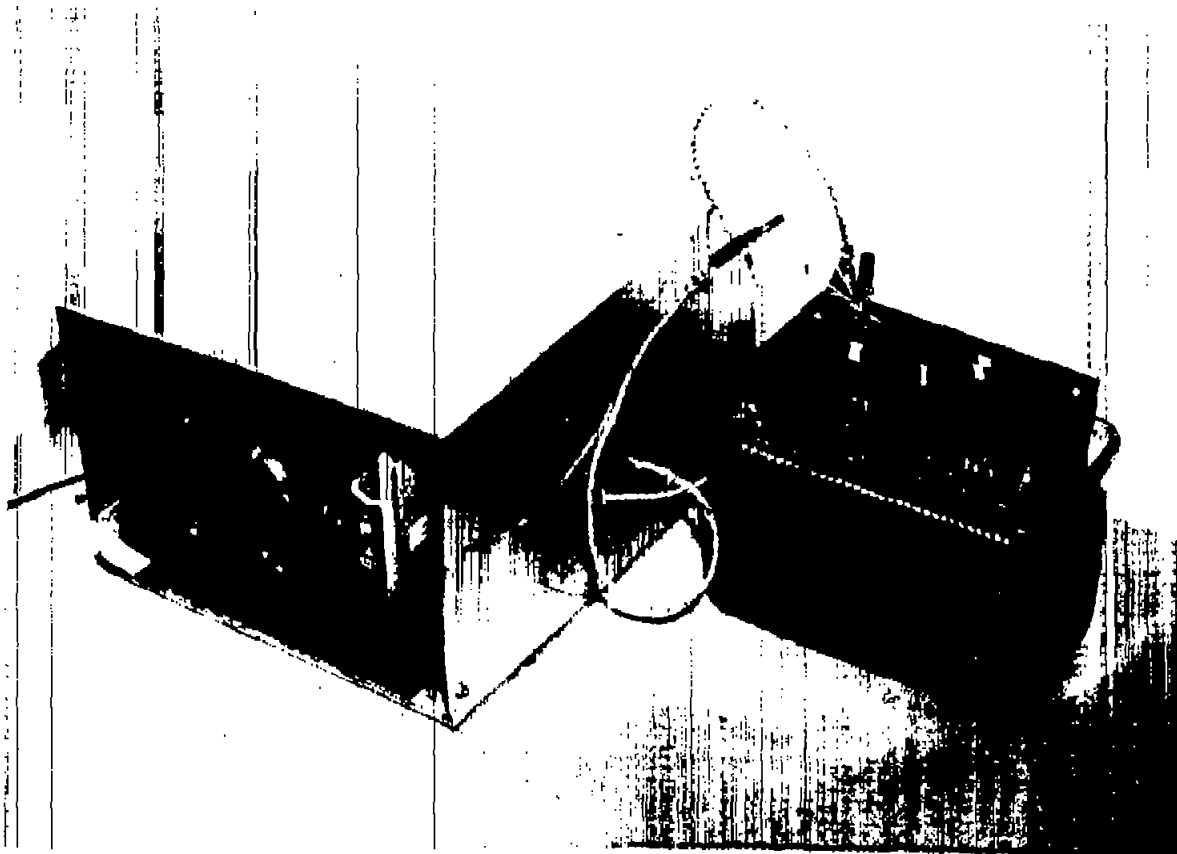


Figure 12.- Plating tank and power supply. L-92487

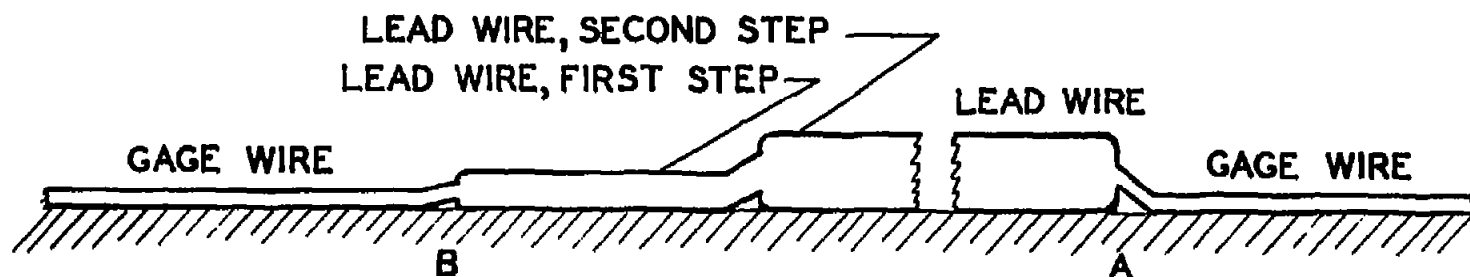


Figure 13.- Schematic representation of lead wire junction with gage wire. A, single-step arrangement, not recommended; B, two-step arrangement, recommended.

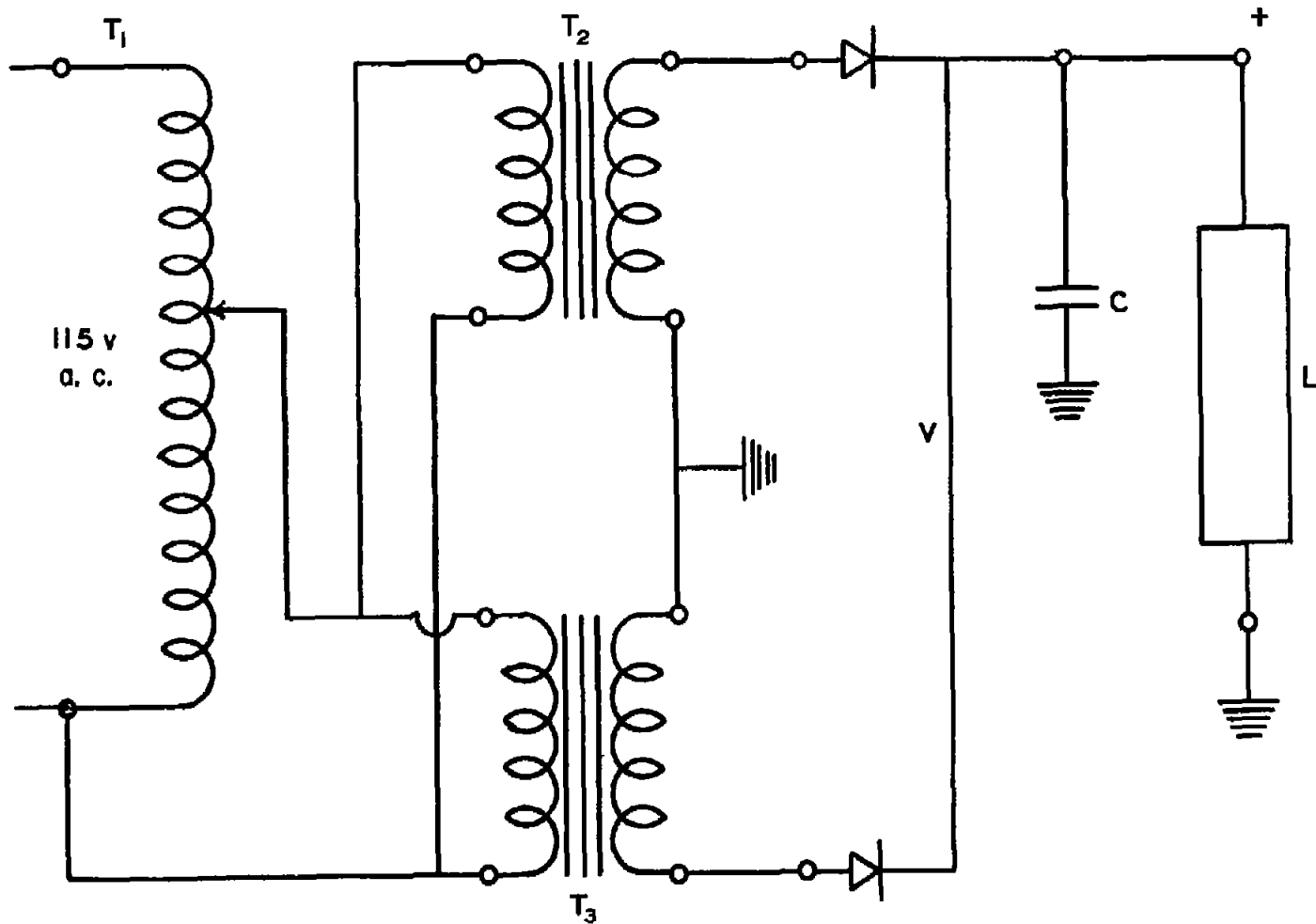


Figure 14.- Diagram of plating circuit.  $T_1$ , variac;  $T_2$  and  $T_3$ , transformers;  $V$ , rectifier;  $C$ , condenser;  $L$ , load.

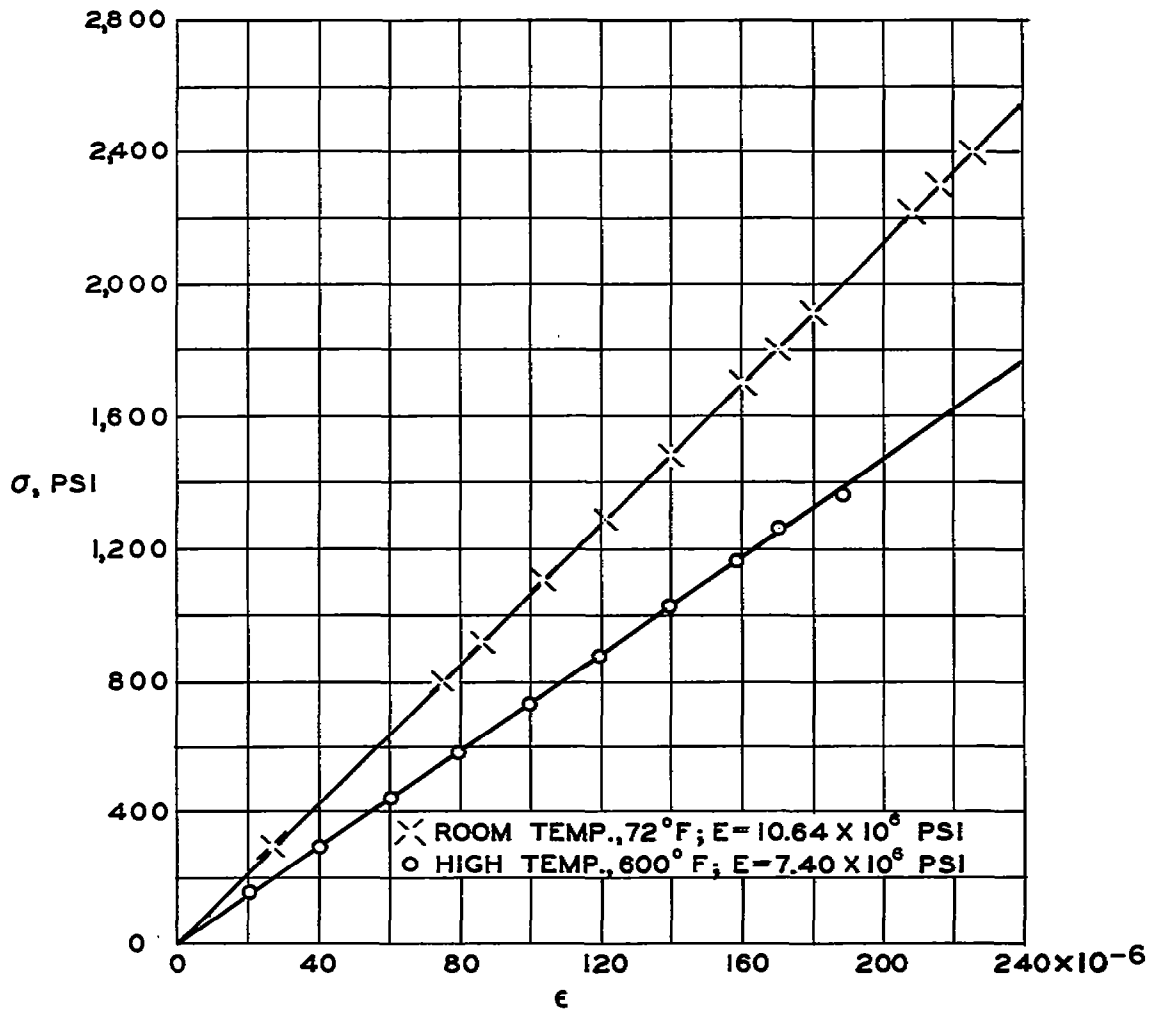


Figure 15.- Experimental stress-strain curve for 2024-T4 aluminum-alloy column (1/2 inch by 1/4 inch by 12 inches).

NASA Technical Library



3 1176 01434 3975